

Gluon condensate in charmonium sum rules with 3-loop corrections

B.L. Ioffe and K.N. Zyablyuk

ioffe@vitep1.itep.ru, zyablyuk@heron.itep.ru

*Institute of Theoretical and Experimental Physics,
B.Cheremushkinskaya 25, Moscow 117218, Russia*

Abstract

Charmonium sum rules are analyzed with the primary goal to obtain the restrictions on the value of dimension 4 gluon condensate. The moments $M_n(Q^2)$ of the polarization operator of vector charm currents are calculated and compared with experimental data. The 3-loop (α_s^2) perturbative corrections, the gluon condensate contribution with α_s corrections and dimension 6 operator G^3 contribution are accounted. It is shown that the sum rules for the moments do not work at $Q^2 = 0$, where the perturbation series diverges and G^3 contribution is large. The domain in the plane (n, Q^2) , where the sum rules are legitimate, is found. Strong correlation of the values of gluon condensate and $\overline{\text{MS}}$ charm quark mass quark is determined. The absolute limits are found to be for gluon condensate $\langle \frac{\alpha_s}{\pi} G^2 \rangle = 0.009 \pm 0.007 \text{ GeV}^4$ and for charm quark mass $\bar{m}(\bar{m}) = 1.275 \pm 0.015 \text{ GeV}$ in $\overline{\text{MS}}$ scheme.

PACS: 14.65.Dw, 11.55.Hx, 12.38.Bx

1 Introduction

It is well known, that QCD vacuum generates various quark and gluon condensates, the vacuum expectation values of quark and gluon fields of nonperturbative origin. Among them the gluon condensate $\langle \frac{\alpha_s}{\pi} G_{\mu\nu}^a G_{\mu\nu}^a \rangle$, where $G_{\mu\nu}^a$ is the gluon field strength tensor and $\alpha_s = \frac{g_s^2}{4\pi}$ is the running QCD coupling constant, plays a special role. The existence of the gluon condensate in QCD was first demonstrated by Shifman, Vainstein and Zakharov [1]. Its special role is caused by few reasons. First, it has the lowest dimension $d = 4$ among gluon condensates, as well as any other condensates conserving chirality. For this reason the gluon condensate is the most important one in determination of hadronic properties by QCD sum rules, if chirality conserving amplitudes are considered (e.g. in case of meson mass determination). Second, the value of the gluon condensate is directly related to the vacuum energy density ε . As was shown in [1]

$$\varepsilon = -\frac{\pi}{8\alpha_s^2} \beta(\alpha_s) \left\langle \frac{\alpha_s}{\pi} G_{\mu\nu}^a G_{\mu\nu}^a \right\rangle \quad (1)$$

where $\beta(\alpha_s)$ is Gell-Mann-Low β -function. Therefore, the sign and magnitude of $\langle \frac{\alpha_s}{\pi} G^2 \rangle$ are very important for theoretical description of QCD vacuum and for construction of hadron models (e.g. the bag model). Third, in some models the numerical value of the gluon condensate is usually used as normalization scale, which fixes the model parameters. For example, in the instanton model it is required, that this value is reproduced by the model.

The numerical value of the gluon condensate

$$\left\langle \frac{\alpha_s}{\pi} G_{\mu\nu}^a G_{\mu\nu}^a \right\rangle = 0.012 \text{ GeV}^4 \quad (2)$$

has been found in [1] from charmonium sum rules. (This value is often referred to as the standard or SVZ value.) Later there were many attempts to determine the gluon condensate by considering various processes within various approaches. In some of them the value (2) (or ones, by a factor of 1.5 higher) was confirmed [2]–[6], in others it was claimed, that the actual value of the gluon condensate is by a factor 2–5 higher than (2) [7]–[14].

From today's point of view the calculations performed in [1] have a serious drawback. Only the first order (NLO) perturbative correction was accounted in [1] and it was taken rather low value of α_s , later not confirmed by the experimental data. (It was assumed, that QCD parameter $\Lambda^{(3)} \approx 100 \text{ MeV}$ and $\alpha_s(m_c) \approx 0.2$, today's values are essentially higher.) The contribution of the next, dimension 6, operator G^3 was neglected, so the convergence of the operator product expansion was not tested. In charmonium sum rules the moments $M_n(Q^2)$ of the polarization function $\Pi(q^2)$, $q^2 = -Q^2$ were calculated at the point $Q^2 = 0$. It was shown in [14], that the higher order terms of the operator product expansion (OPE), namely the contributions of G^3 and G^4 operators are of importance at $Q^2 = 0$. The results of calculations of the second order (NNLO) perturbative corrections to $\Pi(q^2)$ as well as α_s -correction to the gluon condensate are available now. They demonstrate, that both of them as a rule are large and by no means can be neglected in the sum rules for the moments at $Q^2 = 0$. Finally, the experimental data shifted significantly in comparison with ones, used in [1].

Later the charmonium sum rules were considered at the NLO level in [2] for $Q^2 > 0$ and their analysis basically confirmed the results of [1]. There are recent publications [15], [16], [17] where the charmonium as well as bottomonium sum rules were analyzed at $Q^2 = 0$ with α_s^2 perturbative corrections in order to extract the charm and bottom quark masses in various schemes. The condensate is usually taken to be 0 or some another fixed value. However, the charm mass and the condensate values are entangled in the sum rules. This can be easily understood for large Q^2 , where the mass and condensate corrections to the polarization operator behave as some series in negative powers of Q^2 , and one may eliminate the condensate contribution to a great extent by slightly changing the quark mass. Vice versa, different condensate values may vary the charm quark mass within few percents.

The condensate could be also determined from other sum rules, which do not involve the charm quark mass, but the accuracy usually appears to be rather low for this purpose. In particular, precise analysis of e^+e^- data [18] lead only to rather weak restrictions on the gluon condensate. In ref [19] the thorough analysis of hadronic τ -decay structure functions was performed and the restriction $\langle \frac{\alpha_s}{\pi} G^2 \rangle = 0.006 \pm 0.012 \text{ GeV}^4$ was found. This value, however, does not exclude zero value of the condensate.

For all these reasons a reconsideration of the problem is necessary. The charmonium sum rules on the next level of precision in comparison with [1] is presented below. In Section 2

general outline of the method is given and the experimental input data for the sum rules are presented. In Section 3 the method of calculation of the perturbative part of the moments is exposed with the references to the sources, we used in the calculations. Section 4 presents the gluon condensate contribution with α_s -corrections in the form, convenient for numerical evaluation of the moments for nonzero Q^2 . In section 5 perturbative and operator product expansion of the moments is considered. It is argued, that the choice of pole charm quark mass as a mass parameter is not suitable, since in this case the higher order in α_s terms overwhelm the lower ones and the α_s -series are divergent. It is proposed to get rid of this problem by using the $\overline{\text{MS}}$ mass as the mass parameter. In what follows the $\overline{\text{MS}}$ charm quark mass $\bar{m}(\bar{m})$ at the renormalization point equal to the mass itself is used. The formulae for moments $\bar{M}_n(Q^2)$, expressed through the $\overline{\text{MS}}$ mass, are given and the domain in (n, Q^2) plane was found by direct calculation, where the perturbative series are well convergent. In Section 6 the calculation of $\bar{m}(\bar{m})$ and gluon condensate is presented. In Section 7 the sensitivity of the results to the G^3 operator contribution is tested. Section 8 is devoted to the discussion of the attempts to sum up the Coulomb-like corrections. Section 9 contains the conclusion.

2 Experimental current correlator

Consider the 2-point correlator of the vector charm currents:

$$i \int dx e^{iqx} \langle T J_\mu(x) J_\nu(0) \rangle = (q_\mu q_\nu - g_{\mu\nu} q^2) \Pi(q^2), \quad J_\mu = \bar{c} \gamma_\mu c \quad (3)$$

The polarization function $\Pi(q^2)$ can be reconstructed by its imaginary part with the help of the dispersion relation:

$$R(s) = 4\pi \text{Im} \Pi(s + i0), \quad \Pi(q^2) = \frac{q^2}{4\pi^2} \int_{4m^2}^{\infty} \frac{R(s) ds}{s(s - q^2)}, \quad (4)$$

we use normalization $R(\infty) = 1$ in the parton model. In the narrow-width approximation $R(s)$ can be represented as the sum of the resonance δ -functions and continuum:

$$R(s) = \frac{3\pi}{Q_c^2 \alpha_{\text{em}}^2(s)} \sum_\psi m_\psi \Gamma_{\psi \rightarrow ee} \delta(s - m_\psi^2) + \theta(s - s_0) \quad (5)$$

where $Q_c = 2/3$ is electric charge of c -quark, $\alpha_{\text{em}}(s)$ is the running electromagnetic coupling:

$$\alpha_{\text{em}}(s) = \frac{\alpha(0)}{1 - \Delta\alpha(s)}, \quad \Delta\alpha(s) = -4\pi\alpha(0)\Pi_{\text{em}}(-s) = \Delta\alpha_{\text{lep}}(s) + \Delta\alpha_{\text{had}}(s). \quad (6)$$

Here $\alpha(0) = 1/137.04$ is the fine structure constant, $\Pi_{\text{em}}(s)$ is the correlator of electromagnetic currents $J_\mu^{\text{em}} = \sum_i Q_i \bar{\psi}_i \gamma_\mu \psi_i$ defined in the same way as (3). As usual, the leptonic contribution to $\Pi_{\text{em}}(s)$ is found by the perturbation theory, while the hadronic contribution has to be determined by numerical integration of experimental e^+e^- (or τ -decay) data. Since $\alpha_{\text{em}}(s)$ weakly changes from one resonance to another, we fix it at $s = m_{J/\psi}^2$ from now on:

$$\Delta\alpha_{\text{lep}}(m_{J/\psi}^2) = 0.016, \quad \Delta\alpha_{\text{had}}(m_{J/\psi}^2) = 0.009, \quad \alpha_{\text{em}}(m_{J/\psi}^2) = 1/133.6$$

The sum in (5) goes over all 6 charmonium states with $J^{PC} = 1^{--}$ [20]:

notation	mass, MeV	$\Gamma_{\psi \rightarrow ee}$, keV
$J/\psi(1S)$	3096.87 ± 0.04	5.26 ± 0.37
$\psi(2S)$	3685.96 ± 0.09	2.19 ± 0.15
$\psi(3770)$	3769.9 ± 2.5	0.26 ± 0.04
$\psi(4040)$	4040 ± 10	0.75 ± 0.15
$\psi(4160)$	4159 ± 20	0.77 ± 0.23
$\psi(4415)$	4415 ± 6	0.47 ± 0.10

The higher part of the spectrum in eq (5) is approximately parametrized by the last term $\theta(s - s_0)$, where the continuum threshold s_0 is estimated as expected position of the next (7-th) resonance.

In order to suppress the contribution of the continuous tail, one considers the derivatives of the polarization function in euclidean region $q^2 = -Q^2 < 0$, the so-called moments:

$$M_n(Q^2) \equiv \frac{4\pi^2}{n!} \left(-\frac{d}{dQ^2} \right)^n \Pi(-Q^2) = \int_{4m^2}^{\infty} \frac{R(s) ds}{(s + Q^2)^{n+1}} \quad (7)$$

The experimental values are calculated with the help of (5):

$$M_n(Q^2) = \frac{27\pi}{4\alpha_{\text{em}}^2} \sum_{\psi=1}^6 \frac{m_{\psi} \Gamma_{\psi \rightarrow ee}}{(m_{\psi}^2 + Q^2)^{n+1}} + \frac{1}{n(s_0 + Q^2)^n} \quad (8)$$

The squared error of the moments (8) is computed as the sum of the squared errors of each term, mainly due to the width error $\Delta\Gamma_{J/\psi \rightarrow ee}$. For the estimation of the continuum contribution we put $s_0 = (4.6 \text{ GeV})^2$. However we shall always use sufficiently high n , so that the last term in (8) is small compared to the resonance contribution and the uncertainty introduced by this term is negligible. (It is convenient to transfer the continuum contribution to the theoretical side of the sum rules.)

The lowest state J/ψ gives maximal contribution to the moments due to the largest width $\Gamma_{J/\psi \rightarrow ee}$, which itself has the error 7%. This error can be eliminated to a great extent, if one considers the ratio of two moments, which in general case can be written in the following form:

$$r(n_1, Q_1^2; n_2, Q_2^2) \equiv \frac{M_{n_1}(Q_1^2)}{M_{n_2}(Q_2^2)} = \frac{(m_1^2 + Q_2^2)^{n_2+1}}{(m_1^2 + Q_1^2)^{n_1+1}} \frac{1 + D_1}{1 + D_2}, \quad (9)$$

where we denoted

$$D_j = \sum_{\psi=2}^6 D_{j\psi}, \quad D_{j\psi} = \frac{m_{\psi} \Gamma_{\psi}}{m_1 \Gamma_1} \left(\frac{m_1^2 + Q_j^2}{m_{\psi}^2 + Q_j^2} \right)^{n_j+1}$$

the lowest J/ψ state is enumerated by 1. Then the error of this ratio is calculated by usual rules:

$$\left(\frac{\Delta r}{r} \right)^2 = \sum_{j=1}^2 \left(\frac{\Delta D_j}{1 + D_j} \right)^2, \quad (\Delta D_j)^2 = \left(D_j \frac{\Delta \Gamma_1}{\Gamma_1} \right)^2 + \sum_{\psi=2}^6 \left(D_{j\psi} \frac{\Delta \Gamma_{\psi}}{\Gamma_{\psi}} \right)^2 \quad (10)$$

where the mass errors are neglected. If $D_{1,2} \ll 1$, the relative error of the ratio is much smaller than the relative errors of the moments itself. This fact has been utilized in many papers on charmonium sum rules and will be used here.

3 Theoretical $R(s)$

At first one defines the running QCD coupling $a(\mu^2) \equiv \alpha_s(\mu^2)/\pi$ as a solution of the renormalization group equation:

$$\int_{a(\mu_0^2)}^{a(\mu^2)} \frac{da}{\beta(a)} = -\ln \frac{\mu^2}{\mu_0^2}, \quad \beta(a) = \sum_{n \geq 0} \beta_n a^{n+2} \quad (11)$$

Then the functions $R^{(n)}(s, \mu^2)$ are defined as the coefficients in the α_s -expansion:

$$R(s) = \sum_{n \geq 0} R^{(n)}(s, \mu^2) a^n(\mu^2) \quad (12)$$

Since $R(s)$ is the physical quantity, it does not depend on the scale μ^2 , although each term in (12) may be μ^2 dependent.

It is easier to represent the results in terms of the pole quark mass m and the velocity $v = \sqrt{1 - 4m^2/s}$. The first two terms in the expansion (12) do not depend on μ^2 . The leading term $R^{(0)}$ was calculated in [21], the next to leading $R^{(1)}$ in [22]:

$$\begin{aligned} R^{(0)} &= \frac{v}{2}(3 - v^2) \\ R^{(1)} &= \frac{v}{2}(5 - 3v^2) + 2v(3 - v^2) \left(\ln \frac{1 - v^2}{4} - \frac{4}{3} \ln v \right) + \frac{v^4}{3} \ln \frac{1 + v}{1 - v} + \frac{4}{3}(3 - v^2)(1 + v^2) \\ &\quad \times \left[2 \text{Li}_2 \left(\frac{1 - v}{1 + v} \right) + \text{Li}_2 \left(-\frac{1 - v}{1 + v} \right) + \left(\frac{3}{2} \ln \frac{1 + v}{2} - \ln v + \frac{11}{16} \right) \ln \frac{1 + v}{1 - v} \right] \end{aligned} \quad (13)$$

where $\text{Li}_2(x) = \sum_{n=1}^{\infty} \frac{x^n}{n^2}$ is the dilogarithm function. The function $R^{(2)}$ is usually decomposed into four gauge invariant terms:

$$R^{(2)} = C_F^2 R_A^{(2)} + C_A C_F R_{NA}^{(2)} + C_F T n_l R_l^{(2)} + C_F T R_F^{(2)}, \quad (14)$$

where $C_A = 3$, $C_F = 4/3$, $T = 1/2$ are group factors, $n_l = n_f - 1$ is the number of light quarks. The function $R_l^{(2)}$ comes from the diagram with two quark loops: one loop with massive quark, which couples to the vector currents, and another massless quark loop (the so-called double bubble diagram). It was originally found in [23] and in our normalization takes the form:

$$R_l^{(2)} = \left(-\frac{1}{4} \ln \frac{\mu^2}{4s} - \frac{5}{12} \right) R^{(1)} + \delta^{(2)} \quad (15)$$

where the function $\delta^{(2)}$ is given by equation (B.3) in ref [24]. The function $R_F^{(2)}$ comes from the similar double bubble diagram with equal quark masses and has the form [25]:

$$R_F^{(2)} = \rho^V + \rho^R - \frac{1}{4} R^{(1)} \ln \frac{\mu^2}{m^2} \quad (16)$$

where ρ^V is given by equation (12) in ref [25]. The function ρ^R comes from the 4-particle cut and vanishes for $s < 16m^2$. It is represented as the double integral (13) in ref [25] which

can be computed numerically. However for $s > 16 m^2$ the total function $R_F^{(2)}$ can be well approximated by its high energy asymptotic:

$$R_F^{(2)} = -\frac{1}{4} R^{(1)} \ln \frac{\mu^2}{s} + \zeta_3 - \frac{11}{8} - \frac{13}{2} \frac{m^2}{s} + O(m^4/s^2) \quad (17)$$

In numerical calculations we take all the terms up to m^{12}/s^6 , extracted from [26]. The functions $R_A^{(2)}$ and $R_{NA}^{(2)}$ are generated by the diagrams with single quark loop and various gluon exchanges, $R_A^{(2)}$ is abelian part while $R_{NA}^{(2)}$ contains purely nonabelian contributions. They are not known analytically. We will use the approximations, given by equations (65), (66) in ref [24] (divided by 3 in our conventions) which reproduce all known asymptotics and Pade approximations with high accuracy.

4 Condensate contribution

The contribution of the dimension 4 gluon condensate $\langle aG^2 \rangle \equiv \langle \frac{\alpha_s}{\pi} G_{\mu\nu}^a G_{\mu\nu}^a \rangle$ to the polarization function of massive quarks has the form:

$$\Pi^{(G)}(-Q^2) = \frac{\langle aG^2 \rangle}{(4m^2)^2} [f^{(0)}(z) + a f^{(1)}(z)] , \quad \text{where} \quad z = \frac{-Q^2}{4m^2} ,$$

The leading order function was found in [1]:

$$f^{(0)}(z) = -\frac{1}{12 z^4 v^4} \left[\frac{3}{8} \frac{2z-1}{zv} \ln \frac{v-1}{v+1} + z^2 - z + \frac{3}{4} \right] , \quad (18)$$

where $v = \sqrt{1 - 1/z}$. For this function the following dispersion-like relation can be written:

$$f^{(0)}(z) = -\frac{1}{12} \int_1^\infty \frac{dz'}{z'^3 v'} \left[\frac{3}{4} \frac{1}{(z'-z)^2} + \frac{z'}{(z'-z)^3} \right] \quad (19)$$

This representation is convenient for an evaluation of various transformations of the polarization function $\Pi(s)$, in particular, the moments.

The next-to-leading order function $f^{(1)}$ was explicitly found in [12]. One could differentiate it n times to obtain the moments for arbitrary Q^2 . However, we prefer to construct the dispersion integral similar to (19). The function $f^{(1)}(z)$ has a cut from $z = 1$ to ∞ and behaves as v^{-6} at $z \rightarrow 1$. Integrating $f^{(1)}(z')/(z'-z)$ by z' along the contour around the cut, one obtains the following representation:

$$\begin{aligned} f^{(1)}(z) = & \frac{1}{\pi} \int_{1+\epsilon}^\infty \frac{\text{Im } f^{(1)}(z'+i0)}{z'-z} dz' + \sum_{i=1}^3 \frac{\pi^2 f_i}{(1-z)^i} - \frac{65}{1152} \frac{\epsilon^{-3/2}}{1-z} \\ & + \left[\frac{8633}{6912} + \frac{17}{36} \ln(8\epsilon) \right] \frac{\epsilon^{-1/2}}{1-z} + \frac{65}{384} \frac{\epsilon^{-1/2}}{(1-z)^2} \end{aligned} \quad (20)$$

where $\epsilon \rightarrow 0$ and

$$f_1 = -\frac{17}{384} , \quad f_2 = -\frac{413}{6912} , \quad f_3 = -\frac{197}{2304} \quad (21)$$

The imaginary part is:

$$\text{Im } f^{(1)}(z + i0) = \frac{\pi}{96z^5v^5} \left[P_2^V(z) + \frac{P_3^V(z)}{zv} \ln \frac{1-v}{1+v} + P_4^V(z)(1-z) \left(2 \ln v + \frac{3}{2} \ln(4z) \right) \right] \quad (22)$$

where the polynomials $P_i^V(z)$ are given in the Table 1 of ref [12]. It behaves as v^{-5} at $z \rightarrow 1$, so the integral in (20) is divergent in the limit $\epsilon \rightarrow 0$. We decompose it into 3 parts

$$\frac{1}{\pi} \text{Im } f^{(1)}(z + i0) = F_1(z) + F_2'(z) + \frac{1}{2} F_3''(z) \quad (23)$$

in such way, that each function $F_i(z)$ behaves as v^{-1} at $z \rightarrow 1$ and has appropriate asymptotic at $z \rightarrow \infty$. In particular we choose

$$\begin{aligned} F_1(z) &= \frac{1}{96z^4v} \left[\frac{1627}{36} + \frac{893}{9}z - \frac{98}{3}z^2 + 368z^3 \right. \\ &\quad + \left(\frac{89}{6} - 22z - \frac{140}{3}z^2 + \frac{3208}{3}z^3 - 3232z^4 + 2208z^5 \right) \frac{1}{zv} \ln \frac{1-v}{1+v} \\ &\quad \left. + \left(68z + \frac{1688}{9}z^2 - \frac{4256}{3}z^3 + 1472z^4 \right) \left(2 \ln v + \frac{3}{2} \ln(4z) \right) \right] \\ F_2(z) &= \frac{1}{96z^4v} \left[-\frac{23}{4} + \frac{559}{18}z + \frac{272}{3}z^2 + \left(-\frac{197}{8} + \frac{947}{72}z \right) \frac{1}{zv} \ln \frac{1-v}{1+v} \right. \\ &\quad \left. + \frac{136}{3}z^2 \left(2 \ln v + \frac{3}{2} \ln(4z) \right) \right] \\ F_3(z) &= \frac{1}{96z^3v} \left[-\frac{67}{6} - \frac{197}{12} \frac{1-v}{zv} \ln \frac{1-v}{1+v} \right] \end{aligned} \quad (24)$$

Then one may integrate (20) by parts twice and all singular in ϵ term cancel. Eventually we obtain following representation for the function $f^{(1)}$:

$$f^{(1)}(z) = \sum_{i=1}^3 \left[\frac{\pi^2 f_i}{(1-z)^i} + \int_1^\infty \frac{F_i(z')}{(z'-z)^i} dz' \right] \quad (25)$$

It will be used to compute the moments numerically.

5 Moments in $\overline{\text{MS}}$ scheme

For definiteness let us choose the scale $\mu^2 = m^2$ in (12) and write down the α_s -expansion of the moments (7):

$$M_n(Q^2) = \sum_{k \geq 0} M_n^{(k)}(Q^2) a^k(m^2) + \left\langle \frac{\alpha_s}{\pi} G^2 \right\rangle \sum_{k \geq 0} M_n^{(G,k)}(Q^2) a^k(m^2) \quad (26)$$

The perturbative coefficient functions are:

$$M_n^{(k)}(Q^2) = \int_{4m^2}^\infty \frac{R_n^{(k)}(s, m^2) ds}{(s + Q^2)^{n+1}} \quad (27)$$

The leading order can be expressed via Gauss hypergeometric function:

$$M_n^{(0)}(Q^2) = \frac{1}{(4m^2)^n} \frac{3\sqrt{\pi}}{4} \frac{(n+1)\Gamma(n)}{\Gamma(n+5/2)} {}_2F_1\left(\begin{matrix} n, n+2 \\ n+5/2 \end{matrix} \middle| -\frac{Q^2}{4m^2}\right) \quad (28)$$

The higher order functions $M^{(1)}$ and $M^{(2)}$ are computed numerically by (27). (Notice, that the analytical expression for $M_n^{(1)}(0)$ has been found in [15] and the first 7 moments $M_n^{(2)}(0)$ can be determined from the low energy expansion of the polarization function $\Pi(s)$ available in [24].)

The leading order contribution of the gluon condensate is easily obtained from (19):

$$M_n^{(G,0)}(Q^2) = -\frac{\pi^2}{(4m^2)^{n+2}} \frac{\sqrt{\pi}}{6} \frac{(n+1)\Gamma(n+4)}{\Gamma(n+7/2)} {}_2F_1\left(\begin{matrix} n+2, n+4 \\ n+7/2 \end{matrix} \middle| -\frac{Q^2}{4m^2}\right) \quad (29)$$

The next-to-leading condensate correction can be computed numerically with the help of the integral representation, obtained from (25):

$$M_n^{(G,1)}(Q^2) = \frac{4\pi^2}{(4m^2)^{n+2}} \sum_{i=1}^3 \frac{\Gamma(n+i)}{\Gamma(n+1)\Gamma(i)} \left[\frac{\pi^2 f_i}{(1+y)^{n+i}} + \int_1^\infty \frac{F_i(z)}{(z+y)^{n+i}} dz \right], \quad (30)$$

where $y = Q^2/(4m^2)$, the constants f_i and the functions $F_i(z)$ are given in (21) and (24).

The pole quark mass m is the most natural choice, since it is the physical invariant. However in the pole scheme the perturbative corrections to the moments are huge. For instance, at the typical point, which will be used later in our analysis, one gets:

$$n = 10, Q^2 = 4m^2 : \quad \frac{M^{(1)}}{M^{(0)}} = 13.836, \quad \frac{M^{(2)}}{M^{(0)}} = 193.33, \quad \frac{M^{(G,1)}}{M^{(G,0)}} = 13.791 \quad (31)$$

Since in the domain of interest $a \sim 0.1$, this is an indication, that the series (26) is divergent. The situation is even worse for $Q^2 = 0$ (see [15]). It is almost impossible to choose an informative region in the (n, Q^2) plane where the perturbative corrections in the pole mass scheme are tolerable and the continuum as well as $\langle G^3 \rangle$ contributions are suppressed enough on the other hand.

The traditional solution to this problem is the mass redefinition. In particular, in the most popular $\overline{\text{MS}}$ scheme the mass corrections are known to be significantly smaller. In $\overline{\text{MS}}$ conventions the mass \bar{m} depends on the scale μ^2 according to the RG equation:

$$\bar{m}(\mu^2) = \bar{m}(\mu_0^2) \exp\left(\int_{a(\mu_0^2)}^{a(\mu^2)} \frac{\gamma_m(a)}{\beta(a)} da\right), \quad \gamma_m(a) = \sum_{n \geq 0} \gamma_n a^{n+1}, \quad (32)$$

where γ_m is the mass anomalous dimension. In what follows we shall choose the most natural mass scale $\mu^2 = \bar{m}^2$ and will denote $\bar{m}(\bar{m}^2)$ as simply \bar{m} .

There is a perturbative relation between the pole mass m and $\overline{\text{MS}}$ one \bar{m} :

$$\frac{m^2}{\bar{m}^2} = 1 + \sum_{n \geq 1} K_n a^n (\bar{m}^2) \quad (33)$$

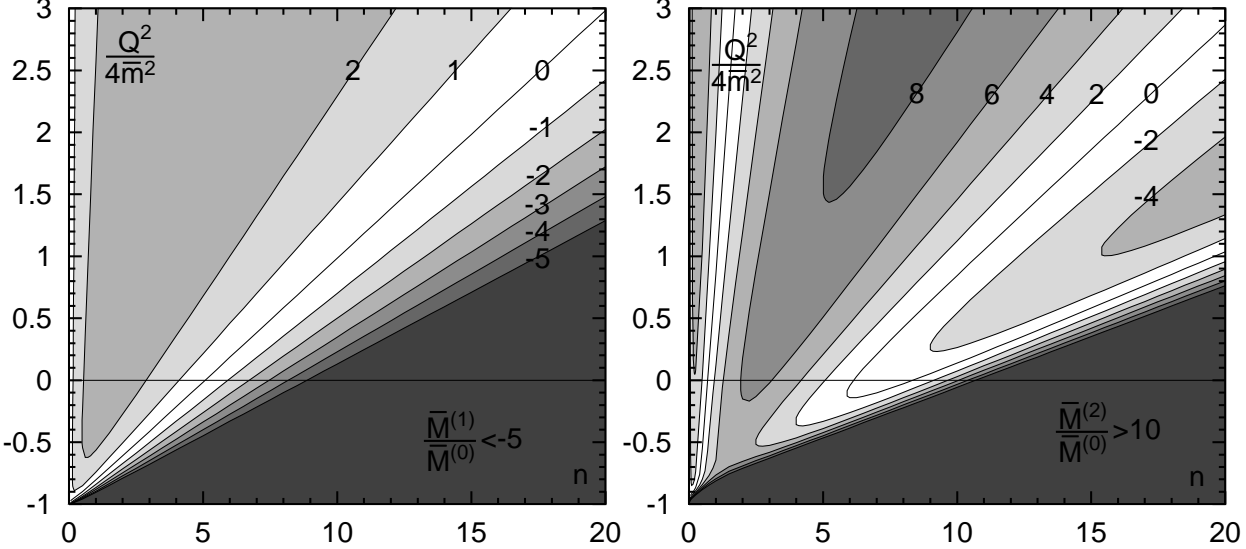


Figure 1: Ratio $\bar{M}_n^{(1)}/\bar{M}_n^{(0)}$ (left) and $\bar{M}_n^{(2)}/\bar{M}_n^{(0)}$ (right) in the plane (n, Q^2) .

The 2-loop factor was found, in particular, in [27], while the 3-loop factor was recently calculated in [28]:

$$\begin{aligned}
 K_1 &= \frac{8}{3} \\
 K_2 &= 28.6646 - 2.0828 n_l = 22.4162 \\
 K_3 &= 417.039 - 56.0871 n_l + 1.3054 n_l^2 = 260.526
 \end{aligned} \tag{34}$$

We put $n_l = 3$ in the last column. The series (33) also looks divergent at the charm scale. (Notice, that the authors of [1] used another mass convention, although numerically close to $\overline{\text{MS}}$ scheme at the NLO level: the coefficient K_1 was equal to $4 \ln 2$ there.)

Nevertheless let us assume for a moment, that α_s is small, take advantage of (33,34) and express the moments (7) in terms of the mass \bar{m} :

$$M_n(Q^2) = \sum_{k \geq 0} \bar{M}_n^{(k)}(Q^2) a^k(\bar{m}^2) + \left\langle \frac{\alpha_s}{\pi} G^2 \right\rangle \sum_{k \geq 0} \bar{M}_n^{(G,k)}(Q^2) a^k(\bar{m}^2) \tag{35}$$

As follows from the definition (7) and dimensional consideration

$$\begin{aligned}
 \bar{M}_n^{(0)}(Q^2) &= M_n^{(0)} \\
 \bar{M}_n^{(1)}(Q^2) &= M_n^{(1)} - K_1(n - d/2) M_n^{(0)} + K_1(n + 1) Q^2 M_{n+1}^{(0)} \\
 \bar{M}_n^{(2)}(Q^2) &= M_n^{(2)} - K_1(n - d/2) M_n^{(1)} + K_1(n + 1) Q^2 M_{n+1}^{(1)} \\
 &\quad + (n - d/2) \left[\frac{K_1^2}{2} (n + 1 - d/2) - K_2 \right] M_n^{(0)} \\
 &\quad + (n + 1) [K_2 - K_1^2(n + 1 - d/2)] Q^2 M_{n+1}^{(0)} + \frac{K_1^2}{2} (n + 1)(n + 2) Q^4 M_{n+2}^{(0)} \\
 \bar{M}_n^{(G,0)}(Q^2) &= M_n^{(G,0)} \\
 \bar{M}_n^{(G,1)}(Q^2) &= M_n^{(G,1)} - K_1(n + 2 - d/2) M_n^{(G,0)} + K_1(n + 1) Q^2 M_{n+1}^{(G,0)}
 \end{aligned} \tag{36}$$

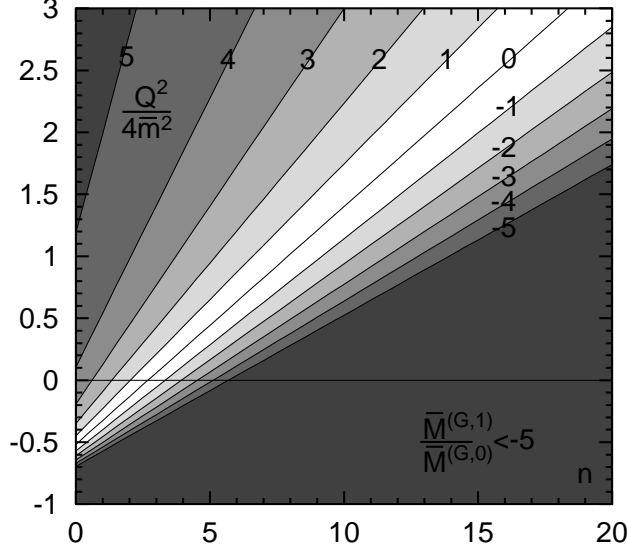


Figure 2: Ratio $\bar{M}_n^{(G,1)}/\bar{M}_n^{(G,0)}$ in the plane (n, Q^2)

where d is the dimension of the polarization function $\Pi(Q^2)$ ($d = 0$ for vector currents), all $M_n^{(i)}$ in the rhs are computed with $\overline{\text{MS}}$ mass \bar{m} .

The moment corrections $\bar{M}^{(k)}$ are much smaller than $M^{(k)}$ in the pole scheme. In particular, at the same point, which was considered in (31), we have now:

$$n = 10, Q^2 = 4\bar{m}^2 : \quad \frac{\bar{M}^{(1)}}{\bar{M}^{(0)}} = 0.045, \quad \frac{\bar{M}^{(2)}}{\bar{M}^{(0)}} = 1.136, \quad \frac{\bar{M}^{(G,1)}}{\bar{M}^{(G,0)}} = -1.673 \quad (37)$$

This smallness of corrections as compared to the pole scheme is observed for almost all n and Q^2 . The ratios $\bar{M}_n^{(1)}/\bar{M}_n^{(0)}$ and $\bar{M}_n^{(2)}/\bar{M}_n^{(0)}$ are shown in Fig 1 and the ratio $\bar{M}_n^{(G,1)}/\bar{M}_n^{(G,0)}$ in the Fig 2 for $n = 0 \dots 20$ and $Q^2/(4\bar{m}^2) = -1 \dots 3$. The perturbative expansion in $\overline{\text{MS}}$ -scheme obviously does not work in the area of high n and low Q^2 , marked with dark. (The detailed data are presented in the Tables 1,2,3 in the Appendix.)

Now we can argue, why the expression (36) for the moments is legitimate, despite that the series (33), relating the pole mass m and $\overline{\text{MS}}$ mass \bar{m} , is divergent at the coupling α_s taken on the charm mass scale. If α_s is small enough, eq (36) is correct. In this case the same values of \bar{M}_n can be obtained by the procedure, when $\overline{\text{MS}}$ mass renormalization is performed directly in the diagrams, without all the concept of the pole mass. If the pole mass concept is not used, the relations (33,34) are irrelevant. These relations demonstrate only, that the pole mass is an ill defined object in case of charm. The check of selfconsistency of $M_n^{(k)}$ moments is the convergence of the series (35).

If one takes the QCD coupling at some another scale $\alpha_s(\mu^2)$, the function $M^{(2)}$ must be replaced by:

$$a(\bar{m}^2) \rightarrow a(\mu^2), \quad \bar{M}_n^{(2)}(Q^2) \rightarrow \bar{M}_n^{(2)}(Q^2) + \bar{M}_n^{(1)}(Q^2) \beta_0 \ln \frac{\mu^2}{\bar{m}^2} \quad (38)$$

so that the series (35) is μ^2 -independent at the order α_s^2 .

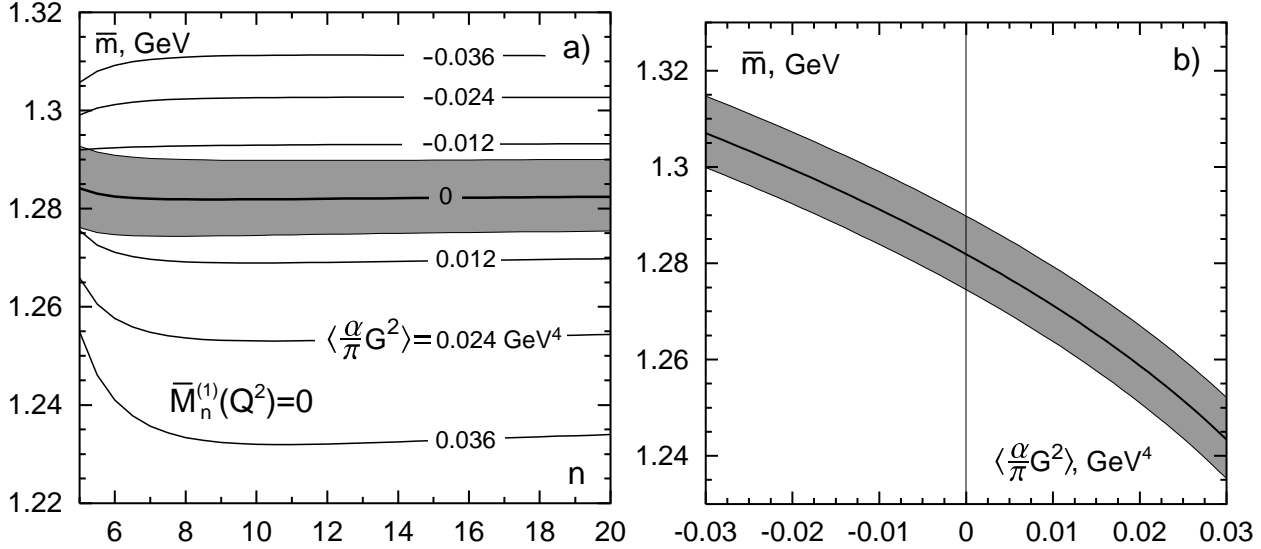


Figure 3: a): $\overline{\text{MS}}$ mass found from experimental moments $M_n(Q_n^2)$ for different n and Q_n^2 determined by the equation $\bar{M}_n^{(1)}(Q_n^2) = 0$ for different values of the gluon condensate. The shaded area shows the experimental error for $\langle \frac{\alpha_s}{\pi} G^2 \rangle = 0$, for nonzero condensates only the central lines are shown. b): $\bar{m}(\bar{m}^2)$ in GeV vs $\langle \frac{\alpha_s}{\pi} G^2 \rangle$ in GeV^4 determined from $n = 10$ and $Q^2 = 0.98 \times 4\bar{m}^2$. The α_s is taken at the scale (40).

6 Determination of charm quark mass and gluon condensate from data

Theoretical moments depend on 3 parameters: charm quark mass, QCD coupling constant and gluon condensate. The QCD coupling α_s is universal quantity and can be taken from other experiments. In particular, as boundary condition in the RG equation (11) we put:

$$\alpha_s(m_\tau^2) = 0.330 \pm 0.025, \quad m_\tau = 1.777 \text{ GeV} \quad (39)$$

found from hadronic τ -decay analysis [19] at the τ -mass in agreement with other data [20].

Another question is the choice of the scale μ^2 , at which α_s should be taken. Since the higher order perturbative corrections are not known, the moments $M_n(Q^2)$ will depend on this scale. In the massless limit the most natural choice is $\mu^2 = Q^2$. On the other hand for massive quarks and $Q^2 = 0$ the scale is usually taken $\mu^2 \sim m^2$. So we choose the interpolation formula:

$$\mu^2 = Q^2 + \bar{m}^2 \quad (40)$$

At this scale α_s is smaller than at $\mu^2 = \bar{m}^2$ for the price of larger $\bar{M}_n^{(2)}$ according to (38). (Notice, that in the Tables in the Appendix as well as in the Fig 1 the ratio $\bar{M}^{(2)}/\bar{M}^{(0)}$ is given at the scale $\mu^2 = \bar{m}^2$.) Sometimes we will vary the coefficient before \bar{m}^2 (40) to test the dependence of the results on the scale.

As the Fig 2 demonstrates, the α_s correction to the gluon condensate is large at $Q^2 = 0$. The $\langle G^3 \rangle$ condensate contribution is also large (see below), which demonstrates, that the operator product expansion is divergent here. For these reasons we will avoid using the sum rules at small Q^2 .

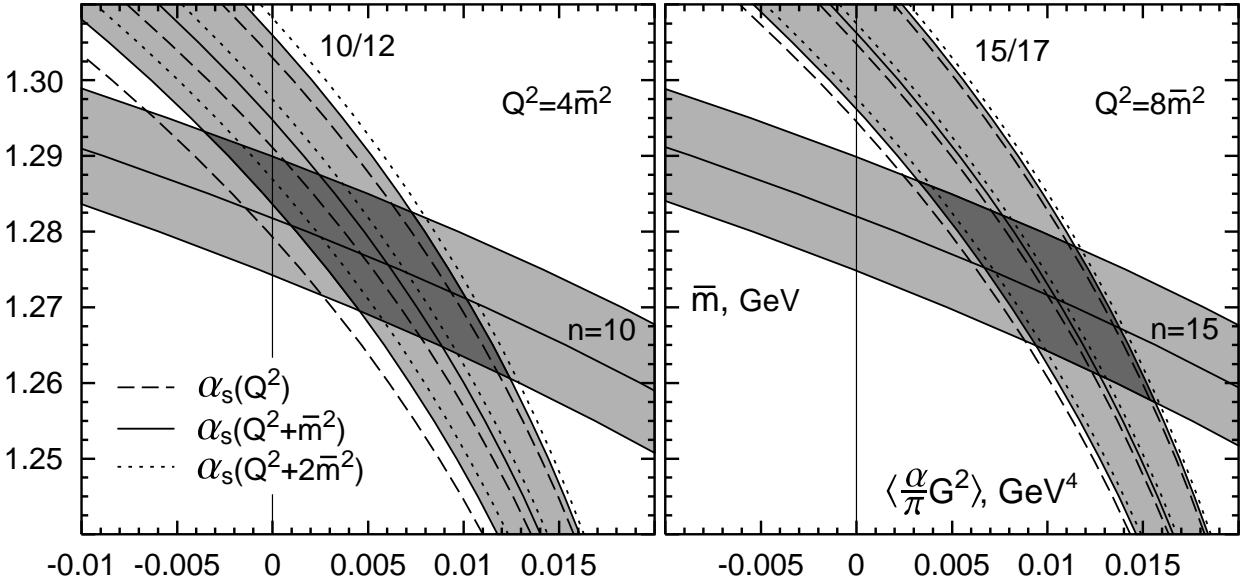


Figure 4: $\overline{\text{MS}}$ mass versus gluon condensate obtained from different points on (n, Q^2) plane. "Horizontal" bands obtained from the moments $(10, 4\bar{m}^2)$ and $(15, 8\bar{m}^2)$, "vertical" bands obtained from the ratio of the moments M_{10}/M_{12} (left), M_{15}/M_{17} (right) for few different choices of $\alpha_s(\mu^2)$.

As the Fig 1 shows, the first correction to the moments $\bar{M}_n^{(1)}(Q^2)$ vanishes along the diagonal line, approximately parametrized by the equation $Q^2/(4\bar{m}^2) = n/5 - 1$. The second-order correction $\bar{M}^{(2)}$ and the correction to the condensate contribution $\bar{M}^{(G,1)}$ are also small along this diagonal for $n > 5$. Now let us compare the theoretical moments with experimental value (8) at different points on this diagonal. If the condensate is fixed, then one can numerically solve this equation in order to find the $\overline{\text{MS}}$ mass. The result is shown in Fig 3a. The values $n < 5$ are not reliable, since the α_s -correction to the condensate exceeds -50% here.

The lines in Fig 3a are almost horizontal, if the condensate is not too large. Consequently there is a correlation between the mass and condensate and we establish the dependence of the $\overline{\text{MS}}$ charm mass \bar{m} on the condensate $\langle \frac{\alpha_s}{\pi} G^2 \rangle$ found at the point $n = 10$, $Q^2 = 0.98 \times 4\bar{m}^2$ on this diagonal. It is plotted in the fig 3b. The error of the experimental moments is about 7%, arising mainly from the uncertainty in $\Gamma_{J/\psi \rightarrow ee}$. But, since $M_n(Q^2) \sim (4\bar{m}^2 + Q^2)^{-n}$, the mass error is of order $7/n\%$, i.e. is much smaller. For instance, at zero condensate

$$\bar{m}(\bar{m}^2) = 1.283 \pm 0.007 \text{ GeV} \quad \text{for} \quad \left\langle \frac{\alpha_s}{\pi} G^2 \right\rangle = 0 \quad (41)$$

the error is purely experimental. The dependence plotted in fig 3b as well as the value (41) are weakly sensitive to particular choice of the QCD coupling α_s and the scale μ^2 . This is an obvious advantage of nonzero Q^2 while the analysis at $Q^2 = 0$ leads to significantly higher error [17].

It is more difficult to find the restrictions on the mass and condensate separately. For this purpose one has to choose the point in (n, Q^2) plane which is 1) out of the diagonal, since no new information can be obtained from there, 2) not in the lower right corner (high n , low Q^2),

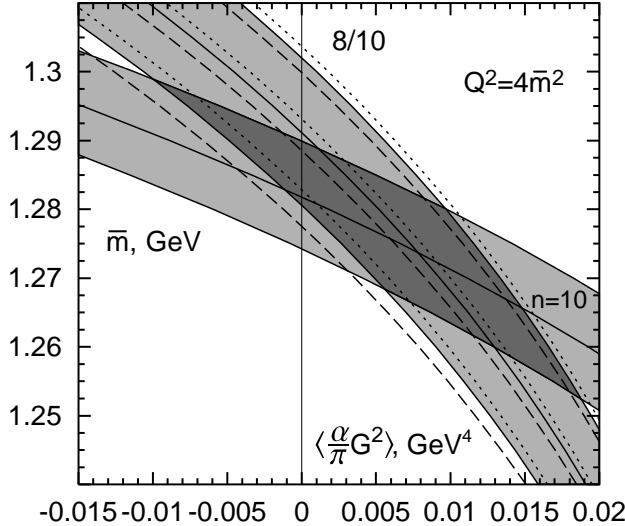


Figure 5: $\overline{\text{MS}}$ mass versus gluon condensate obtained from the ratio M_8/M_{10} above the diagonal. For more notations see Fig 4.

where perturbative corrections as well as α_s corrections to the gluon condensate are large and 3) not in the upper left corner (low n , high Q^2), where the continuum contribution to the experimental moments is uncontrollable. It turns out that if one considers the ratio of the moments (9), the mass–condensate dependence appears to be different in comparison to the fig 3b. In particular, the results obtained from the ratio M_{10}/M_{12} at $Q^2 = 4\bar{m}^2$ and M_{15}/M_{17} at $Q^2 = 8\bar{m}^2$ are demonstrated in the left and right parts of the Fig 4 respectively. At the same figures the mass-condensate dependence, obtained from the moments $M_{10}(Q^2 = 4\bar{m}^2)$ and $M_{15}(Q^2 = 8\bar{m}^2)$ is also plotted. The error bands include both the experimental error of the ratio (10) and the uncertainty of α_s (39). Obviously the results, obtained outside the diagonal, are sensitive to the choice of α_s as well as μ^2 . The small variation of μ^2 slightly changes the acceptable region in the fig 4, but if one takes μ^2 few times lower, the region expands to the left significantly.

The absolute limits of the $\overline{\text{MS}}$ charm quark mass and the gluon condensate can be determined from the fig 4:

$$\bar{m}(\bar{m}^2) = 1.275 \pm 0.015 \text{ GeV} , \quad \left\langle \frac{\alpha_s}{\pi} G^2 \right\rangle = 0.009 \pm 0.007 \text{ GeV}^4 \quad (42)$$

The restrictions on \bar{m} and the gluon condensate, obtained from other ratios of moments, agree with (42), but are weaker (see Fig 5, where the ratio M_8/M_{10} is considered).

$R(s)$ in (12), or the expression for the moments are, in principle, independent on the normalization scale μ^2 . However, in fact, since we take into account only first 3 terms in the α_s -expansion in (26), such dependence takes place. Namely, when we change the normalization point from \bar{m}^2 to $\mu^2 = Q^2 + \bar{m}^2$ (40) with the help of eq (38), the values of the moments, defined by (26), are changed. As is clear from (38), the difference between the moments $M_n(Q^2)$ at the normalization points \bar{m}^2 and $Q^2 + \bar{m}^2$ increases with Q^2 . At Q^2 used above, the difference is moderate and, if recalculated to $\left\langle \frac{\alpha_s}{\pi} G^2 \right\rangle$, results in the error $\Delta \left\langle \frac{\alpha_s}{\pi} G^2 \right\rangle \sim 2 \times 10^{-3} \text{ GeV}^4$, much smaller, than the overall error in (42). However, going to

the higher Q^2 would be dangerous. In fact, while deriving (38), we expanded the running QCD coupling $a(\mu^2)$ in $a(\bar{m}^2)$. This expansion is valid if

$$a \beta_0 \ln \frac{Q^2}{\bar{m}^2} \ll 1 \quad (43)$$

In particular for $Q^2/(4\bar{m}^2) = 3$ the l.h.s. of this equation is ~ 0.5 and the neglected higher order terms could be significant. For this reason we avoid to use higher Q^2 , than it was done.

Let us now turn the problem around and try to predict the width $\Gamma_{J/\psi \rightarrow ee}$ theoretically. In order to avoid the wrong circle argumentation we do not use the condensate value just obtained, but take the limitation $\langle \frac{\alpha_s}{\pi} G^2 \rangle = 0.006 \pm 0.012 \text{ GeV}^4$ found in [19] from τ -decay data. Then, the mass limits $\bar{m} = 1.28 - 1.33 \text{ GeV}$ can be found from the moments exhibited above which do not depend on $\Gamma_{J/\psi \rightarrow ee}$ with very good precision ($\lesssim 3\%$). The substitution of these values of \bar{m} into the moments gives

$$\Gamma_{J/\psi \rightarrow ee}^{\text{theor}} = 4.9 \pm 0.8 \text{ keV} \quad (44)$$

in comparison with experimental value $\Gamma_{J/\psi \rightarrow ee} = 5.26 \pm 0.37 \text{ keV}$. Such good coincidence of the theoretical prediction and experimental data is a very impressive demonstration of the QCD sum rules effectiveness. It must be stressed, that while obtaining (44) no additional input were used besides the condensate restriction taken from [19] and the value of $\alpha_s(m_\tau^2)$.

7 $D = 6$ condensate influence

The $D = 4$ gluon condensate $\langle aG^2 \rangle$ is the leading term in the operator expansion series. The question arises, how the higher dimension condensate could change the results of our analysis. There is single $D = 6$ gluon condensate $\langle g^3 G^3 \rangle$. Its contribution to the polarization function (3) can be parametrized as follows:

$$\Pi^{(G3)}(s) = \frac{\langle g^3 f^{abc} G_{\mu\nu}^a G_{\nu\lambda}^b G_{\lambda\mu}^c \rangle}{(4m^2)^3} f^{(G3)}(z), \quad z = \frac{s}{4m^2},$$

The dimensionless function $f^{(G3)}(z)$ has been found in [29]:

$$f^{(G3)}(z) = -\frac{1}{72\pi^2 z^3} \left(\frac{2}{15} + \frac{2}{5}z + 4J_2 - \frac{31}{3}J_3 + \frac{43}{5}J_4 - \frac{12}{5}J_5 \right), \quad (45)$$

where the integrals

$$J_n = \int_0^1 \frac{dx}{[1 - 4zx(1 - x)]^n}$$

can be calculated analytically. However the integral representation is convenient to express the result in terms of Gauss hypergeometric function, which can be easily differentiated in order to obtain the moments:

$$M_n(Q^2) = M_n^{(0)}(Q^2) + \dots + \langle g^3 f^{abc} G_{\mu\nu}^a G_{\nu\lambda}^b G_{\lambda\mu}^c \rangle M_n^{(G3)}(Q^2), \quad (46)$$

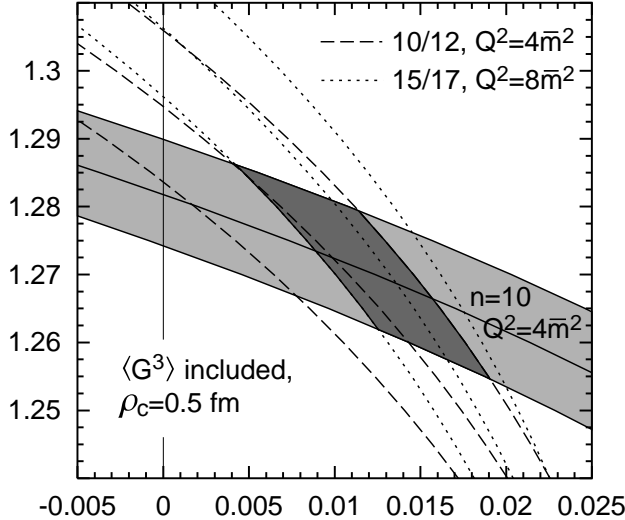


Figure 6: $\overline{\text{MS}}$ mass versus gluon condensate obtained from the moments and ratios with account of $\langle G^3 \rangle$ condensate according to (47).

where

$$M_n^{(G^3)}(Q^2) = \frac{\sqrt{\pi}}{1080 (4m^2)^{n+3}} \sum_{i=2}^4 c_i \frac{\Gamma(n+i) \Gamma(n+5)}{\Gamma(n+1) \Gamma(n+9/2)} {}_2F_1\left(\begin{array}{c} n+i, n+5 \\ n+9/2 \end{array} \middle| -\frac{Q^2}{4m^2}\right)$$

and the constants $c_2 = 3$, $c_3 = -7$, $c_4 = -9$. Significance of the condensate $\langle g^3 G^3 \rangle$ is determined by the ratio of the two terms in (46). The numerical values of this ratio for different (n, Q^2) are given in the last column of the Tables 1,2,3 in the Appendix.

No reliable estimations of the $\langle G^3 \rangle$ condensate are available. There exists only the estimation, based on the dilute instanton gas model [30]:

$$\langle g^3 f^{abc} G_{\mu\nu}^a G_{\nu\lambda}^b G_{\lambda\mu}^c \rangle = \frac{4}{5} \frac{12\pi^2}{\rho_c^2} \left\langle \frac{\alpha_s}{\pi} G^2 \right\rangle, \quad (47)$$

where ρ_c is effective instanton radius. The numerical value of ρ_c is uncertain, even in the framework of the model: in [31] the value $\rho_c = 1/3 \text{ fm} = 1.5 \text{ GeV}^{-1}$ was advocated, in [1] the value $\rho_c = 1 \text{ fm} = 4.5 \text{ GeV}^{-1}$ was used. In the recent paper [32], based on the sensitive to gluon condensate sum rules, $\rho_c = 0.5 \text{ fm} = 2.5 \text{ GeV}^{-1}$ was suggested.

The contribution of $\langle g^3 G^3 \rangle$ to $M_n(Q^2)$ at a fixed n falls rapidly with growth of Q^2 . At $Q^2 = 0$ and $n \geq 5$ it comprises about 50% or more of the gluon condensate contribution at $\rho_c = 0.5 \text{ fm}$. Even at $Q^2/(4\bar{m}^2) = 1$ it is significant: the (negative) correction to the gluon condensate term is $\sim 10\%$ in M_{10} and $\sim 30\%$ in the ratio M_{10}/M_{12} . One gets more reliable results at $Q^2/(4\bar{m}^2) = 2$. Here the corrections are: -7% for M_{15} and -18% for M_{15}/M_{17} . These corrections leave the charm quark mass almost unchanged, but increase the gluon condensate and its error (compare Figs 4 and 6). The account of $\langle g^3 G^3 \rangle$ contribution leads to the following restriction:

$$\left\langle \frac{\alpha_s}{\pi} G^2 \right\rangle = 0.011 \pm 0.009 \text{ GeV}^4 \quad (48)$$

Certainly, it relies upon the instanton gas model, that gives (47).

8 About the attempts to sum up the Coulomb-like corrections

Sometimes when considering of the heavy quarkonia sum rules the Coulomb-like corrections are summed up [15], [25], [33], [34], [35]. The basic argumentation for such summation is that at $Q^2 = 0$ and high n only small quark velocities $v \lesssim 1/\sqrt{n}$ are essential and the problem becomes nonrelativistic. So it is possible to perform the summation with the help of well known formulae of nonrelativistic quantum mechanics for $|\psi(0)|^2$ in case of Coulomb interaction (see [36]).

We do not use this method in our case for the following reasons:

1. The basic idea of our approach is to calculate the moments of the polarization operator in QCD by applying the perturbation theory and OPE (l.h.s. of the sum rules) and to compare it with the r.h.s. of the sum rules, represented by the contribution of charmonium states (mainly by J/ψ). Therefore it is assumed, that the theoretical side of the sum rule is dual to experimental one, i.e. the same domains of coordinate and momentum spaces are of importance at both sides. But the charmonium states (particularly, J/ψ) are by no means the Coulomb systems. A particular argument in favor of this statement is the ratio $\Gamma_{J/\psi \rightarrow ee}/\Gamma_{\psi' \rightarrow ee} = 2.4$. If charmonia were nonrelativistic Coulomb system, $\Gamma_{\psi \rightarrow ee}$ would be proportional to $|\psi(0)|^2 \sim 1/(n_r + 1)^3$, and since ψ' is the first radial excitation with $n_r = 1$, this ratio would be equal to 8.

2. The heavy quark-antiquark Coulomb interaction at large distances $r > R_{\text{conf}} \sim 1 \text{ GeV}^{-1}$ is screened by gluon and light quark-antiquark clouds, resulting in string formation. Therefore the summation of Coulombic series makes sense only when the Coulomb radius R_{Coul} is below R_{conf} . (It must be taken in mind, that higher order terms in Coulombic series represent the contributions of large distances, $r \gg R_{\text{Coul}}$.) For charmonia we have

$$R_{\text{Coul}} \approx \frac{2}{m_c C_F \alpha_s} \approx 4 \text{ GeV}^{-1}$$

It is clear, that the necessary condition $R_{\text{Coul}} < R_{\text{conf}}$ is badly violated for charmonia. (Even for bottomonium $R_{\text{Coul}} \approx R_{\text{conf}}$.) This means that the summation of the Coulomb series in case of charmonium would be a wrong step.

3. Our analysis is performed at $Q^2/4\bar{m}^2 \geq 1$. It is easy to estimate from (7), that for typical values of our analysis $n = 10$, $Q^2 = 4\bar{m}^2$ the characteristic domain of the quark velocities is $v \sim 0.4$. It is hard to expect the validity of the nonrelativistic formulae here. The momentum transfer from quark to antiquark in this case can be estimated as $\Delta p \lesssim 1.3 \text{ GeV}$. (This is typical domain for QCD sum rule validity.) In coordinate space it corresponds to $\Delta r_{q\bar{q}} \gtrsim 0.8 \text{ GeV}^{-1}$. Comparison with potential models [37] demonstrates, that in this region the effective potential strongly differs from Coulombic one.

4. Large compensation of various terms in the expression for the moments in $\overline{\text{MS}}$ scheme (see Fig 1) is not achieved, if only the Coulomb terms are taken into account. This means, that the terms of non-Coulombic origin are more important here, than Coulombic ones.

For all these reasons we believe, that the summation of nonrelativistic Coulomb corrections is inadequate in the problem in view: it will not improve the accuracy of calculations, but would be misleading.

9 Results and discussion

The analysis of charmonium sum rules is performed within the framework of QCD at the next level of precision in comparison with famous treatment of this problem by Shifman, Vainstein and Zakharov [1]. In the perturbation theory the terms of order α_s^2 were accounted as well as α_s corrections to the gluon condensate contribution, in OPE — the dimension 6 operator G^3 . The method of the moments was exploited. The validity of the method was demonstrated for the $\overline{\text{MS}}$ mass of the charm quark, but not for the pole mass. The domain in the plane (n, Q^2) was found, where the three accounted terms in the perturbative series are well converging. It was shown, that the sum rules do not work at $Q^2 = 0$, where the following 3 requirements cannot be satisfied simultaneously: 1) convergence of the perturbation series, 2) small α_s correction to the gluon condensate contribution, 3) small contribution of G^3 operator. The most suitable values of Q^2 for the sum rules are $Q^2 \sim (1-2)4\bar{m}^2 \sim 5-15 \text{ GeV}^2$. The values of charmed quark $\overline{\text{MS}}$ and the gluon condensate were found by comparing the theoretical moments with experimental ones, saturated by charmonium resonances (plus continuum). A strong correlation of the values \bar{m} and $\langle \frac{\alpha_s}{\pi} G^2 \rangle$ was established. This connection only weakly depends on α_s . Taking the α_s value found in [19] from hadronic τ -decay data

$$\alpha_s(m_\tau^2) = 0.330 \pm 0.025, \quad (49)$$

the $\overline{\text{MS}}$ charm quark mass and the gluon condensate were determined

$$\bar{m}(\bar{m}^2) = 1.275 \pm 0.015 \text{ GeV}, \quad \left\langle \frac{\alpha_s}{\pi} G^2 \right\rangle = 0.009 \pm 0.007 \text{ GeV}^4 \quad (50)$$

The error in (50) roughly comprises as 50% theoretical (uncertainty in α_s and the normalization scale) and 50% experimental (mainly the error of J/ψ electronic decay width). The numbers in (50) were obtained disregarding the contribution of G^3 operator. The account of G^3 term, when $\langle G^3 \rangle$ was taken using the dilute instanton gas model with $\rho_c = 0.5 \text{ fm}$, shifts (50) to

$$\left\langle \frac{\alpha_s}{\pi} G^2 \right\rangle = 0.011 \pm 0.009 \text{ GeV}^4 \quad (51)$$

The value (51) may be compared with recently found [19] limitation on the gluon condensate from hadronic τ -decay data:

$$\left\langle \frac{\alpha_s}{\pi} G^2 \right\rangle = 0.006 \pm 0.012 \text{ GeV}^4 \quad (52)$$

Eqs (51) and (52) are compatible and obtained from independent sources. So, with some courage, we can average them and get

$$\left\langle \frac{\alpha_s}{\pi} G^2 \right\rangle_{\text{av}} = 0.0085 \pm 0.0075 \text{ GeV}^4 \quad (53)$$

After such averaging we come back to (50).

We can formulate our final conclusion about the gluon condensate value in such a way. The values of gluon condensate two times (or more) larger than the SVZ value (2) are certainly excluded. Unfortunately our analysis does not allow to exclude zero values of

the gluon condensate. In this aspect the improvement of the experimental precision of $J/\psi \rightarrow e^+e^-$ width would be helpful. Based on the condensate limitation (52) and the value of α_s (49), the J/ψ electronic decay width $\Gamma_{J/\psi \rightarrow ee}$ was predicted theoretically:

$$\Gamma_{J/\psi \rightarrow ee}^{\text{theor}} = 4.9 \pm 0.8 \text{ keV} \quad (54)$$

in comparison with the experimental value $5.26 \pm 0.37 \text{ keV}$. Such a good coincidence ones more demonstrates the effectiveness of QCD sum rule approach.

Acknowledgement

Authors thank A.I. Vainstein and K.G. Chetyrkin for fruitful discussions.

The research described in this publication was made possible in part by Award No RP2-2247 of U.S. Civilian Research and Development Foundation for Independent States of Former Soviet Union (CRDF), by the Russian Found of Basic Research grant 00-02-17808 and INTAS grant 2000, project 587.

References

- [1] M.A. Shifman, A.I. Vainstein, and V.I. Zakharov, Nucl. Phys. **B147** (1979) 385; 448
- [2] L.J. Reinders, H.R. Rubinstein, and S. Yazaki, Nucl. Phys. **B186** (1981) 109
- [3] S. Narison, "QCD Spectral Sum Rules", World Scientific, 1989; Phys. Lett. **B387** (1996) 162
- [4] V.A. Novikov, M.A. Shifman, A.I. Vainstein, M.B. Voloshin, and V.I. Zakharov, Nucl. Phys. **B237** (1984) 525
- [5] S.I. Eidelman, L.M. Kurdadze, and A.I. Vainstein, Phys. Lett. **B82** (1979) 278
- [6] K.J. Miller and M.G. Olsson, Phys. Rev. **D25** (1982) 1247
- [7] R.A. Bertlmann, Nucl. Phys. **B204** (1982) 387
- [8] V.N. Baier, and Yu.F. Pinelis, Phys. Lett. **B116** (1982) 179; Nucl. Phys. **B229** (1983) 29
- [9] G. Launer, S. Narison, and R. Tarrach, Z. Phys. **C26** (1984) 433
- [10] R.A. Bertlmann, C.A. Domingues, M. Loewe, M. Perrottet, and E. de Rafael, Z. Phys. **C39** (1988) 231
- [11] P.A. Baikov, V.A. Ilyin, and V.A. Smirnov, Phys. Atom. Nucl. **56** (1993) 1527
- [12] D.J. Broadhurst, P.A. Baikov, V.A. Ilyin, J. Fleischer, O.V. Tarasov, and V.A. Smirnov, Phys. Lett. **B329** (1994) 103

- [13] B.V. Geshkenbein, Phys. Atom. Nucl. **59** (1996) 289
- [14] S.N. Nikolaev, and A.V. Radyushkin, JETP Lett. **37** (1982) 526
- [15] M. Jamin and A. Pich, Nucl. Phys. **B507** (1997) 334
- [16] M. Eidemuller and M. Jamin, Phys. Lett. **B498** (2001) 203
- [17] J.H. Kuhn and M. Steinhauser, Nucl. Phys. **B619** (2001) 588
- [18] S. Eidelman, E. Jergenlehner, A.L. Kataev, and O. Veretin, Phys. Lett. **B454** (1999) 369
- [19] B.V. Geshkenbein, B.L. Ioffe, and K.N. Zyablyuk, Phys. Rev. **D64** (2001) 093009
- [20] K. Hagiwara et al. (Particle Data Group), Phys. Rev. **D66** (2002) 010001
- [21] V.B. Berestetski and I.Ya. Pomeranchuk, Sov. Phys. JETF **29** (1955) 864
- [22] J. Schwinger, "Particles, sources and fields", Vol. 2, Addison-Wesley Publ., 1973
- [23] A.H. Hoang, J.H. Kuhn, and T. Teubner, Nucl. Phys. **B452** (1995) 173
- [24] K.G. Chetyrkin, J.H. Kuhn, and M. Steinhauser, Nucl. Phys. **B482** (1996) 213
- [25] K.G. Chetyrkin, A.H. Hoang, J.H. Kuhn, M. Steinhauser, and T. Teubner, Eur. Phys. J. **C2** (1998) 137
- [26] K.G. Chetyrkin, R. Harlander, J.H. Kuhn, and M. Steinhauser, Nucl. Phys. **B503** (1997) 339
- [27] N. Gray, D.J. Broadhurst, W. Grafe, and K. Schilcher, Z. Phys. **C48** (1990) 573
- [28] K. Melnikov and T. van Ritbergen, Phys. Lett. **B482** (2000) 99; K.G. Chetyrkin and M. Steinhauser, Nucl. Phys. **B573** (2000) 617
- [29] S.N. Nikolaev and A.V. Radyushkin, Sov. J. Nucl. Phys. **39** (1984) 91
- [30] V.A. Novikov, M.A. Shifman, A.I. Vainstein, and V.I. Zakharov, Phys. Lett. **B86** (1979) 347
- [31] T. Shafer and E.V. Shuryak, Rev. Mod. Phys. **70** (1998) 323
- [32] B.L. Ioffe and A.V. Samsonov, Phys. At. Nucl. **63** (2000) 1448
- [33] V.A. Novikov et al, Phys. Rep. **41** (1978) 1
- [34] M.B. Voloshin, Nucl. Phys. **B154** (1979) 365, Int. J. Mod. Phys. **A10** (1995) 2865
- [35] J.H. Kuhn, A.A. Penin, and A.A. Pivovarov, Nucl. Phys. **B534** (1998) 356
- [36] L. Landau and E. Lifshitz, "Quantum Mechanics: Nonrelativistic Theory", Pergamon Press, 1977
- [37] E. Eichten et al, Phys. Rev. **D21** (1980) 203

Appendix: Numerical values of the moments

We list here the numerical values of the perturbative moments $\bar{M}^{(0,1,2)}$, condensate contribution $\bar{M}^{(G,0,1)}$ in $\overline{\text{MS}}$ scheme computed by (36) and $\langle G^3 \rangle$ condensate contribution $M^{(G3)}$ (46) for $n = 1..20$ and $Q^2/(4\bar{m}^2) = 0, 1, 2$. For dimensionfull values we put $4\bar{m}^2 = 1$ here, so that the leading term $\bar{M}^{(0)}$ and the ratios $\bar{M}^{(G,0)}/\bar{M}^{(0)}$, $\bar{M}^{(G3)}/\bar{M}^{(0)}$ should be divided by $(4\bar{m}^2)^n$ and $(4\bar{m}^2)^2$, $(4\bar{m}^2)^3$ respectively for a particular mass \bar{m} .

n	$\bar{M}_n^{(0)}$	$\bar{M}_n^{(1)}/\bar{M}_n^{(0)}$	$\bar{M}_n^{(2)}/\bar{M}_n^{(0)}$	$\bar{M}_n^{(G,0)}/\bar{M}_n^{(0)}$	$\bar{M}_n^{(G,1)}/\bar{M}_n^{(G,0)}$	$\bar{M}_n^{(G3)}/\bar{M}_n^{(0)}$
1	0.8	2.394	2.384	-15.04	2.477	0.056
2	0.3429	2.427	6.11	-58.49	1.054	0.826
3	0.2032	1.917	6.115	-143.6	-0.484	4.003
4	0.1385	1.1	4.402	-283.4	-2.107	12.76
5	0.1023	0.078	2.162	-491.3	-3.798	32.21
6	7.9565×10^{-2}	-1.092	0.213	-780.3	-5.545	69.81
7	6.4187×10^{-2}	-2.375	-0.836	-1164.	-7.337	135.9
8	5.3207×10^{-2}	-3.75	-0.514	-1654.	-9.17	243.9
9	4.5043×10^{-2}	-5.199	1.559	-2266.	-11.04	411.2
10	3.8776×10^{-2}	-6.711	5.698	-3011.	-12.94	659.1
11	3.3841×10^{-2}	-8.277	12.17	-3903.	-14.86	1014.
12	2.9872×10^{-2}	-9.89	21.19	-4955.	-16.81	1506.
13	2.6624×10^{-2}	-11.54	32.98	-6181.	-18.78	2172.
14	2.3924×10^{-2}	-13.23	47.69	-7593.	-20.77	3055.
15	2.1653×10^{-2}	-14.96	65.49	-9204.	-22.78	4204.
16	1.9719×10^{-2}	-16.71	86.51	-1.103×10^4	-24.81	5673.
17	1.8058×10^{-2}	-18.49	110.9	-1.308×10^4	-26.85	7526.
18	1.6617×10^{-2}	-20.3	138.7	-1.537×10^4	-28.91	9834.
19	1.5359×10^{-2}	-22.13	170.1	-1.791×10^4	-30.98	1.268×10^4
20	1.4252×10^{-2}	-23.98	205.2	-2.072×10^4	-33.07	1.614×10^4

Table 1: Moments at $Q^2 = 0$

n	$\bar{M}_n^{(0)}$	$\bar{M}_n^{(1)}/\bar{M}_n^{(0)}$	$\bar{M}_n^{(2)}/\bar{M}_n^{(0)}$	$\bar{M}_n^{(G,0)}/\bar{M}_n^{(0)}$	$\bar{M}_n^{(G,1)}/\bar{M}_n^{(G,0)}$	$\bar{M}_n^{(G3)}/\bar{M}_n^{(0)}$
1	0.4348	2.235	-0.307	-2.816	4.532	-0.02
2	9.7902×10^{-2}	2.64	4.407	-10.19	4.03	-0.058
3	2.9985×10^{-2}	2.709	6.752	-23.8	3.455	-0.082
4	1.047×10^{-2}	2.588	7.653	-45.32	2.825	-0.014
5	3.9365×10^{-3}	2.34	7.582	-76.4	2.15	0.279
6	1.5529×10^{-3}	1.999	6.85	-118.7	1.438	1.004
7	6.3364×10^{-4}	1.587	5.683	-173.9	0.697	2.452
8	2.6515×10^{-4}	1.118	4.253	-243.5	-0.071	5.015
9	1.1314×10^{-4}	0.601	2.7	-329.4	-0.862	9.197
10	4.9032×10^{-5}	0.045	1.136	-433.	-1.673	15.63
11	2.1523×10^{-5}	-0.546	-0.343	-556.1	-2.501	25.09
12	9.5483×10^{-6}	-1.167	-1.656	-700.3	-3.346	38.5
13	4.2743×10^{-6}	-1.815	-2.732	-867.3	-4.205	56.96
14	1.9283×10^{-6}	-2.486	-3.508	-1059.	-5.078	81.75
15	8.7574×10^{-7}	-3.178	-3.93	-1276.	-5.962	114.4
16	4.0007×10^{-7}	-3.89	-3.948	-1521.	-6.858	156.4
17	1.8372×10^{-7}	-4.62	-3.518	-1795.	-7.764	209.9
18	8.4756×10^{-8}	-5.365	-2.599	-2101.	-8.68	277.
19	3.9264×10^{-8}	-6.126	-1.154	-2439.	-9.605	360.
20	1.8257×10^{-8}	-6.9	0.85	-2811.	-10.54	461.7

Table 2: Moments at $Q^2 = 4\bar{m}^2$

n	$\bar{M}_n^{(0)}$	$\bar{M}_n^{(1)}/\bar{M}_n^{(0)}$	$\bar{M}_n^{(2)}/\bar{M}_n^{(0)}$	$\bar{M}_n^{(G,0)}/\bar{M}_n^{(0)}$	$\bar{M}_n^{(G,1)}/\bar{M}_n^{(G,0)}$	$\bar{M}_n^{(G3)}/\bar{M}_n^{(0)}$
1	0.3005	2.073	-2.016	-1.098	5.002	-8.936×10^{-3}
2	4.6172×10^{-2}	2.531	2.453	-3.825	4.762	-0.03
3	9.589×10^{-3}	2.734	5.208	-8.691	4.468	-0.064
4	2.2613×10^{-3}	2.792	6.909	-16.2	4.131	-0.105
5	5.7274×10^{-4}	2.753	7.853	-26.84	3.761	-0.14
6	1.5191×10^{-4}	2.643	8.229	-41.11	3.364	-0.147
7	4.1621×10^{-5}	2.478	8.167	-59.5	2.942	-0.094
8	1.1682×10^{-5}	2.27	7.769	-82.51	2.501	0.066
9	3.3404×10^{-6}	2.025	7.113	-110.6	2.042	0.393
10	9.6957×10^{-7}	1.749	6.264	-144.3	1.568	0.963
11	2.8488×10^{-7}	1.447	5.276	-184.1	1.08	1.871
12	8.4559×10^{-8}	1.122	4.195	-230.4	0.579	3.233
13	2.5317×10^{-8}	0.776	3.061	-283.9	0.068	5.186
14	7.6361×10^{-9}	0.412	1.909	-344.8	-0.455	7.89
15	2.3181×10^{-9}	0.031	0.77	-413.8	-0.986	11.53
16	7.0768×10^{-10}	-0.364	-0.33	-491.3	-1.527	16.33
17	2.1713×10^{-10}	-0.773	-1.365	-577.8	-2.075	22.52
18	6.6914×10^{-11}	-1.195	-2.313	-673.9	-2.631	30.38
19	2.0704×10^{-11}	-1.628	-3.153	-779.9	-3.194	40.21
20	6.429×10^{-12}	-2.072	-3.867	-896.4	-3.764	52.36

Table 3: Moments at $Q^2 = 8\bar{m}^2$